Structural Engineering and Mechanics, Vol. 32, No. 4 (2009) 501-516
DOI: http://dx.doi.org/10.12989/sem.2009.32.4.501

Large deflections of spatial variable-arc-length elastica under terminal forces

Boonchai Phungpaingam†, Chainarong Athisakul‡ and Somchai Chucheepsakul‡†

Department of Civil Engineering, Faculty of Engineering, King Mongkut's University of Technology Thonburi, Pracha-Utid Rd, Bangmod, Toongkru, 10140, Thailand

(Received November 12, 2007, Accepted May 14, 2009)

Abstract. This paper aims to study the large deflections of variable-arc-length elastica subjected to the terminal forces (e.g., axial force and torque). Based on Kirchhoff's rod theory and with help of Euler parameters, the set of nonlinear governing differential equations which free from the effect of singularity are established together with boundary conditions. The system of nonlinear differential equations is solved by using the shooting method with high accuracy integrator, seventh-eighth order Runge-Kutta with adaptive step-size scheme. The error norm of end conditions is minimized within the prescribed tolerance (10^{-5}). The behavior of VAL elastica is studied by two processes. One is obtained by applying slackening first. After that keeping the slackening as a constant and then the twist angle is varied in subsequent order. The other process is performed by reversing the sequence of loading in the first process. The results are interpreted by observing the load-deflection diagram and the stability properties are predicted via fold rule. From the results, there are many interesting aspects such as snap-through phenomenon, secondary bifurcation point, loop formation, equilibrium configurations and effect of variable-arc-length to behavior of elastica.

Keywords: Kirchhoff's rod; variable-arc-length elastica; large deflections; snap-through phenomenon; Euler parameters; shooting method.

1. Introduction

The first development of three-dimensional elastica was proposed by Kirchhoff 1859. In his work, he showed that the equilibrium equations from his theory akin to the equations of motion of rigid body with a fixed point. This analogy has been called Kirchhoff's kinetic analogy. Later Clebsch 1862 modified the Kirchhoff's rod theory by adding the initial curvatures into the formulation and Love 1892 completed the formulation of Kirchhoff by using the ordinary approximation theory. In 1907, Cosserat and Cosserat 1907 suggested an important theory about Kirchhoff's rod, the director theory, in which material points of rod were described by position vector and directors. These exceptional works developed by the aforementioned researchers are the foundation of many research areas in engineering and technology at present.

† Ph.D. Candidate
‡ Lecturer
‡† Professor, Corresponding author, E-mail: somchai.chu@kmutt.ac.th

In engineering point of view, there are many applications that employ the Kirchhoff's rod theory for solving the practical problems. For the example, in ocean engineering, marine cables can be treated as the rod and the theory of Kirchhoff's rod can be used to solve the problem of cable such as loop formation (Coyne 1990 and Goyal *et al.* 2005) and the stability of the cables under variety of loads and support conditions (Lu *et al.* 1994, 1995 and Benecke and Vuuren 2005). In biomechanics, the stability and shapes of DNA were investigated by using the Kirchhoff's rod theory (Coleman *et al.* 1995, Coleman and Swingon 2000, Goyal *et al.* 2005 and Balaeff *et al.* 2006). In medical device, the Kirchhoff's rod can be applied to study the loop formation of endoscope probe (Katopodes *et al.* 2001) where the initial curvatures have been taken into account.

With these models, the total arc-length can not be varied but, in some applications such as in marine riser, the arc-length of riser can be released for preventing the excessive tension which may damage the riser. However when the riser is over slackened, the riser may form the loop easily. In order to eliminate the loop, the large amount of tension must be applied to the riser and this causes the riser to experience the high bending stress which can also damage the riser. Thus the study about effect of variable-arc-length to the loop formation may give the information to prevent the riser from such circumstance.

The characteristic of total arc-length of rod that can be varied is called variable-arc-length (VAL) rod/elastica. The model of VAL elastica was initiated and developed by Chucheepsakul and Huang 1992, and in the next three years, the name of VAL elastica was arisen in paper of Chucheepsakul *et al*. 1995. Subsequently, many models of VAL elastica have been developed continuously by studying the behavior of elastica under the different load and end conditions and the fluid interaction. For the example, the fluid interaction was considered in Chucheepsakul and Monprapussorn 2000 and by the same authors in 2001. Many types of loads applying to VAL elastica was investigated such as point load by Chucheepsakul *et al*. 1996, Chucheepsakul and Huang 1997 and Wang *et al.* 1997, moments by Chucheepsakul *et al*. 1997, Chucheepsakul *et al*. 1999, follower load by Wang *et al.* 1998 and Chucheepsakul and Phungpaigram 2004 and the uniform self-weight by Pulngern *et al*. 2005. In addition to the hinge end, the various end conditions were also studied such as clamped end (Zhang and Yang 2005) and rotational spring (Wang *et al*. 1997 and Wang *et al*. 1998). However, the study of VAL elastica in the past confined only to the planar elastica, thus the study of VAL elastica in three-dimensional space is of interest for studying the behavior of spatial VAL elastica.

The aim of this paper is to investigate large deflections behavior of spatial VAL elastica without effects of self-contact and Poisson's ratio. One end of the elastica is clamped and the other is placed on a sleeve support. There are two processes for studying this problem. In the first process, the VAL elastica is loaded by axial force until the elastica is deformed by sliding through the sleeve support. After that the VAL elastica is twisted by applying the torque at that the sleeve end. This process is similar to the clamped rod reported in excellent works of Miyazaki and Kondo 1997 and Heijden *et al*. 2003 but different in initial values of axial load because the fixed total arc-length elastica gives the hardening path in load-deflection curve while VAL elastica yields the softening path (see Fig. 1). The other process is performed by applying the twist at the end. Subsequently, by keeping the twist angle as a constant and then the axial force is applied in which the effect of variable-arc-length will be studied in this process.

The solution strategies for solving this kind of problem are stated in many literatures. One is to solve the problem with reference (or fixed) coordinate which yields the complexity in the formulations. Another strategy is the use of local (or attached) coordinate for reducing the

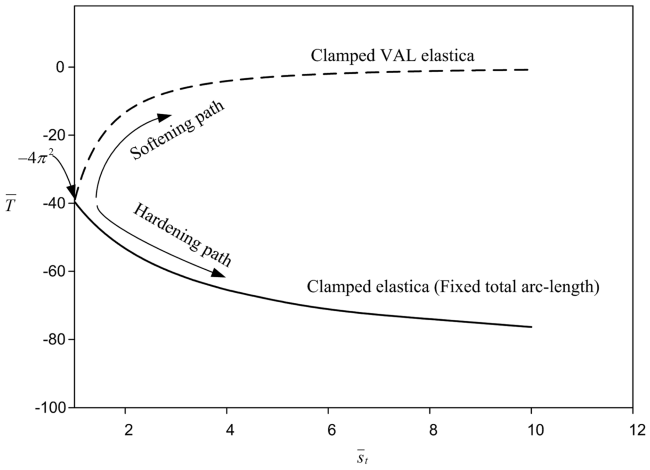

Fig. 1 Equilibrium paths for clamped VAL and fixed total arc-length elastica

complexity of the formulation. Normally, the Euler angles are utilized as the parameters in transformation matrix that maps the coordinate frame from reference coordinate to local coordinate (Benecke and Vuuren 2005, Katopodes *et al*. 2001, Miyazaki and Kondo 1997 and Atanackovic and Glavardanov 2002). However there is a difficulty in formulating the equations using the Euler angles in which the equations contain the singularity during inverse process of transformation matrix. Thus, some researchers (Heijden *et al*. 2003) avoided using the Euler angles but they formulated the equations directly with the unit vectors in local frame. In addition, there also has the transformation matrix involving the four parameters that produces the singularity-free matrix. These four parameters are called Euler parameters (Nikravesh 1988) which is the normalized form of quaternions. Using Euler parameters instead of Euler angles gives not only the singularity-free matrix but also reduces the computational cost since the elements in the matrix are merely polynomial function. Euler parameters were also utilized in work of Balaeff *et al*. 2006 in which they studied the behavior of protein-DNA complexes. In this paper, we take the advantage of Euler parameters for constructing the singularity-free governing differential equations of the problem. After formulating the governing equations, the shooting method is employed to solve the solutions of the problem.

2. Statement of the problem

Considering Fig. 2(a), the naturally straight elastica having uniformly circular cross-section and span length L is clamped at one end and the other is placed on sleeve support that can rotate and slide freely. The flexural and torsional rigidities are EI and GJ, respectively. The applied torque Q and axial force T act at the sleeve end. The unit vectors in reference coordinate are named by $\hat{\mathbf{e}} = (\hat{\mathbf{e}}_1, \hat{\mathbf{e}}_2, \hat{\mathbf{e}}_3)$ in which $\hat{\mathbf{e}}_1$ is directed along the axial line of the rod while $\hat{\mathbf{e}}_2$ and $\hat{\mathbf{e}}_3$ are attached to the principal axes of the elastica. Noting that the symbol for vectors and matrices are bold face letters otherwise they are scalar.

In deformed configuration shown in Fig. 2(b), the total arc-length of the rod is changed from L to

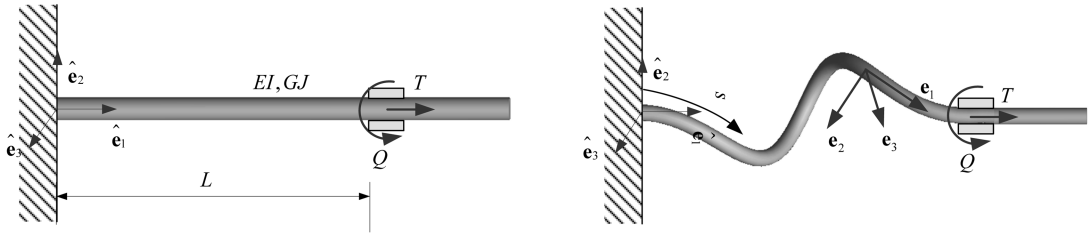

Fig. 2 Variable-arc-length rod: (a) undeformed configuration, (b) deformed configuration

s_t. The unit vectors in local coordinate are introduced as $\mathbf{e} = (\mathbf{e}_1, \mathbf{e}_2, \mathbf{e}_3)$ in which $\mathbf{e}_1$ is oriented to tangential direction of the rod and moved according to the direction of increasing of arc-length s while $\mathbf{e}_2$ and $\mathbf{e}_3$ are still attached to the principal axes of the cross-section.

3. Governing equations

In order to construct the governing differential equations for this problem, the assumption of Kirchhoff 's rod should be made as follows.

- The rod has uniform cross-section and the flexural rigidities of principal axes are equal.
- The material of rod is homogenous and isotropic.
- The dimension of cross-section must be small when compared to the length of rod.
- Axial and shear deformations are neglected.
- The body force and distributed moments are omitted, thus the forces are applied at the end only.
- The applied forces are conservative force.

As it can be seen from Fig. 2(b), the mapping between reference coordinate and local coordinate is necessary. Using the transformation matrix in terms of Euler angles leads to an important drawback which is the occurring of singularity in the formulations. The alternative choice is the use of transformation matrix in terms of Euler parameters $\mathbf{q} = (q_0, q_1, q_2, q_3)$ in which the singularity-free formulation is obtained. In this paper, the governing differential equations are constructed in terms of Euler parameters for obtaining the singularity-free formulations. The transformation matrix in terms of Euler parameters is shown in Eq. (1)

$$\mathbf{U} = \begin{bmatrix} q_0^2 + q_1^2 - 1/2 & q_1 q_2 - q_0 q_3 & q_1 q_3 + q_0 q_2 \\ q_1 q_2 + q_0 q_3 & q_0^2 + q_2^2 - 1/2 & q_2 q_3 - q_0 q_1 \\ q_1 q_3 - q_0 q_2 & q_2 q_3 + q_0 q_1 & q_0^2 + q_3^2 - 1/2 \end{bmatrix} \tag{1}$$

where

$$q_0 = \cos\left(\frac{\phi}{2}\right);\ (q_1, q_2, q_3) = \mathbf{u}\sin\left(\frac{\phi}{2}\right);\ \mathbf{U}^{-1} = \mathbf{U}^T \tag{2a,b,c}$$

The vector $\mathbf{u}$ is the unit vector in direction of rotational axis and ϕ is the rotation of rotational

axis. The global coordinate is rotated into local coordinate by following relation.

$$\mathbf{e} = \mathbf{U}^T \hat{\mathbf{e}} \tag{3}$$

The derivative of Euler parameters with respect to arc-length parameter s in terms of local coordinate is shown below (see Nikravesh 1988).

$$\mathbf{q}' = \frac{1}{2}\mathbf{A}^T \boldsymbol{\omega} \tag{4}$$

where

$$\mathbf{A} = \begin{bmatrix} -q_1 & q_0 & q_3 & -q_2 \\ -q_2 & -q_3 & q_0 & q_1 \\ -q_3 & q_2 & -q_1 & q_0 \end{bmatrix} \tag{5}$$

$$\boldsymbol{\omega} = \omega_1 \mathbf{e}_1 + \omega_2 \mathbf{e}_2 + \omega_3 \mathbf{e}_3 \tag{6}$$

The symbol ( )' stands for the derivative with respect to arc-length parameter s. Eq. (4) gives the relationship between derivative of Euler parameters $\mathbf{q}$ and angular velocity vector $\boldsymbol{\omega}$ where its components are total twist ω_1 and curvatures ω_2 and ω_3. However, each component of angular velocity is difficult to measure. Thus, the components of angular velocity may be changed into the internal torque and moments by using the linear constitutive equation.

The geometric relation of inextensible and unshearable elastica is established via basic concept of differential geometry which is given by

$$\frac{\mathrm{d}\mathbf{r}}{ds} = \mathbf{r}' = x'\hat{\mathbf{e}}_1 + y'\hat{\mathbf{e}}_2 + z'\hat{\mathbf{e}}_3 = \mathbf{e}_1 \tag{7}$$

After the geometric relations are setup, next, the equilibrium equations of rod will be considered. From Fig. 3, the equilibrium equations of rod segment (exclude the body force and distributed moment) are expressed below.

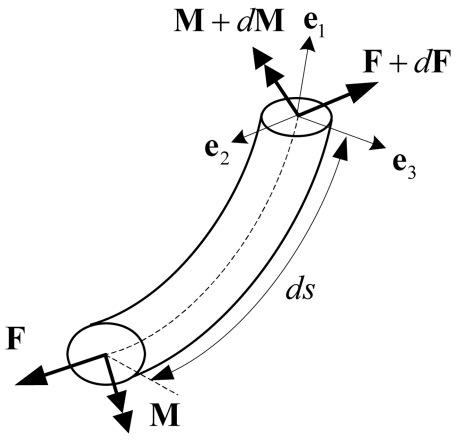

Fig. 3 Rod segment

$$\mathbf{F}' = 0;\ \mathbf{M}' + \mathbf{e}_1 \times \mathbf{F} = 0 \tag{8, 9}$$

The equilibrium equations in Eqs. (8) and (9) are valid for every coordinate system. Based on local coordinate system, the internal forces are defined as $\mathbf{F} = F_1\mathbf{e}_1 + F_2\mathbf{e}_2 + F_3\mathbf{e}_3$ and the internal torque and moments are defined as $\mathbf{M} = M_1\mathbf{e}_1 + M_2\mathbf{e}_2 + M_3\mathbf{e}_3$. The components of internal forces are axial force F_1 and shear forces in principal directions (F_2 and F_3). In the case of internal torque and moments, M_1 represents the internal torque and M_2 and M_3 are bending moments. The axial force F_1 has positive value when it is tension and, for the internal torque M_1, it is positive when it rotates according to the direction of unit vector $\mathbf{e}_1$ (e.g., counterclockwise direction).

As it can be observed in Eqs. (8) and (9), the unit vector of local coordinate must be differentiated with respect to arc-length s. With contribution of Frenet's formulas, the derivative of unit vectors in local frame is governed by following equation.

$$\mathbf{e}_i' = \boldsymbol{\omega} \times \mathbf{e}_i \quad i = 1,2,3 \tag{10}$$

As previous mention, the angular velocity can be changed into the internal torque and moments by using linear constitutive relation, namely.

$$\mathbf{M} = GJ\omega_1\mathbf{e}_1 + EI\omega_2\mathbf{e}_2 + EI\omega_3\mathbf{e}_3 \tag{11}$$

For the sake of generality, the non-dimensional parameters are introduced.

$$\overline{F}_1 = \frac{F_1L^2}{EI},\ \overline{F}_2 = \frac{F_2L^2}{EI},\ \overline{F}_3 = \frac{F_3L^2}{EI},\ \overline{M}_1 = \frac{M_1L}{EI},\ \overline{M}_2 = \frac{M_2L}{EI},\ \overline{M}_3 = \frac{M_3L}{EI} \tag{12a-f}$$

$$\overline{x} = \frac{x}{L},\quad \overline{y} = \frac{y}{L},\quad \overline{z} = \frac{z}{L},\quad \overline{s} = \frac{\tilde{s}}{\overline{s}_t},\quad \tilde{s} = \frac{s}{L},\quad \overline{s}_t = \frac{s_t}{L} \tag{12g-l}$$

$$\overline{T} = \frac{TL^2}{EI},\quad \overline{Q} = \frac{QL}{EI},\quad \alpha = \frac{EI}{GJ} \tag{12m-o}$$

The non-dimensional parameter axial force $\overline{T}$ and torque $\overline{Q}$ are equivalent to the internal force $\overline{F}_1$ and internal torque $\overline{M}_1$ at the boundary. For computational purpose, the vector form of equilibrium equations in Eqs. (8) and (9) must be presented in scalar form by using Eqs. (10), (11) and (12). After some manipulations, the equilibrium equations in non-dimensional form can be rewritten as follows.

$$\overline{F}_1^* = -\overline{s}_t(\overline{F}_3\overline{M}_2 - \overline{F}_2\overline{M}_3) \tag{13}$$

$$\overline{F}_2^* = -\overline{s}_t(\overline{F}_1\overline{M}_3 - \alpha\overline{F}_3\overline{M}_1) \tag{14}$$

$$\overline{F}_3^* = -\overline{s}_t(\alpha\overline{F}_2\overline{M}_1 - \overline{F}_1\overline{M}_2) \tag{15}$$

$$\overline{M}_1^* = 0 \rightarrow \overline{M}_1 = C_1 \tag{16}$$

$$\overline{M}_2^* = -\overline{s}_t\{(1-\alpha)\overline{M}_1\overline{M}_3 - \overline{F}_3\} \tag{17}$$

$$\overline{M}_3^* = \overline{s}_t\{(1-\alpha)\overline{M}_1\overline{M}_2 - \overline{F}_2\} \tag{18}$$

The symbol $(\,)^*$ denotes the derivative with respect to arc-length parameter $\bar{s}$. The stiffness ratio α equals to 1 when the elastica has circular cross-section and the effect of Poisson's ratio is neglected. From Eq. (16), it is clear that torque $\overline{M}_1$ is independent from the arc-length of the rod. Subsequently, the geometric relations in Eqs. (4) and (7) are rewritten in scalar form as

$$q_0^* = \frac{\bar{s}_t}{2}(-q_1\overline{M}_1 - q_2\overline{M}_2 - q_3\overline{M}_3) \tag{19}$$

$$q_1^* = \frac{\bar{s}_t}{2}(q_0\overline{M}_1 - q_3\overline{M}_2 + q_2\overline{M}_3) \tag{20}$$

$$q_2^* = \frac{\bar{s}_t}{2}(q_3\overline{M}_1 + q_0\overline{M}_2 - q_1\overline{M}_3) \tag{21}$$

$$q_3^* = \frac{\bar{s}_t}{2}(-q_2\overline{M}_1 + q_1\overline{M}_2 + q_0\overline{M}_3) \tag{22}$$

$$\bar{x}^* = 2\bar{s}_t(q_0^2 + q_1^2 - 1/2) \tag{23}$$

$$\bar{y}^* = 2\bar{s}_t(q_1q_2 + q_0q_3) \tag{24}$$

$$\bar{z}^* = 2\bar{s}_t(q_1q_3 - q_0q_2) \tag{25}$$

Eqs. (13)-(25) are the set of governing differential equations of this problem.

4. Boundary conditions

The boundary conditions of this problem are listed in Table 1. The angle $\phi(1)$ is the total twist angle at the sleeve end. The unknown parameters that must be evaluated are $\phi(1)$, $\bar{s}_t\overline{F}_1$, $\overline{F}_2, \overline{F}_3, \overline{M}_1, \overline{M}_2$ and $\overline{M}_3$. However, the parameters $\phi(1)$ and $\bar{s}_t$ are set as the controlled parameters. Thus, six unknown parameters are still remained for evaluating. In order to solve the six unknown parameters, the six equations according to the physical characteristics of the problem must be determined. These equations are expressed below.

Table 1 Boundary conditions

Parameters	Boundary values	
	$\bar{s} = 0$	$\bar{s} = 1$
q_0	1	$\cos(\phi(1)/2)$
q_1	0	$\sin(\phi(1)/2)$
q_2	0	0
q_3	0	0
x	0	1
y	0	0
z	0	0

$$f_1 = q_0(1) - \cos(\phi(1)/2) \tag{26}$$

$$f_2 = q_1(1) - \sin(\phi(1)/2) \tag{27}$$

$$f_3 = q_0^2(1) + q_1^2(1) + q_2^2(1) + q_3^2(1) - 1 \tag{28}$$

$$f_4 = \bar{x}(1) - 1 \tag{29}$$

$$f_5 = \bar{y}(1) \tag{30}$$

$$f_6 = \bar{z}(1) \tag{31}$$

Eq. (28) is the identity of the Euler parameters ($\mathbf{q}\mathbf{q}^T = 1$). By using the shooting method the above six equations must be minimized and the solutions of the problem are obtained.

5. Shooting method

The effective tool for solving the two-point boundary value problem, the shooting method, is employed for solving the system of differential equations (Eqs. (13)-(25)) under boundary conditions in Table 1. In this method, we attempt to minimize Eqs. (26)-(31) for each value of controlled parameters $\bar{s}_t$ and $\phi(1)$. The solution steps for evaluating the solutions are summarized as follows:

1. Assign the value to parameters $\phi(1)$ and $\bar{s}_t$, then estimate the values of unknown parameters $\bar{F}_1$, $\bar{F}_2, \bar{F}_3, \bar{M}_1, \bar{M}_2$ and $\bar{M}_3$ for the first iteration.
2. Integrate Eqs. (13)-(25) from $\bar{s} = 0$ to $\bar{s} = 1$ by using seventh-eighth order Runge-Kutta with adaptive step size scheme.
3. Minimize the error of norm in which the objective function for minimization process is

$$\text{Min}\Phi = |f_1| + |f_2| + |f_3| + |f_4| + |f_5| + |f_6| \tag{32}$$

   If the minimization process is successful ($\Phi \le 10^{-5}$), then the solutions of $\bar{F}_1$, $\bar{F}_2, \bar{F}_3, \bar{M}_1, \bar{M}_2$ and $\bar{M}_3$ are obtained. If the minimization process fails, return to step 1 to estimate the unknown parameters.
4. After obtaining the solutions, the controlled parameter $\phi(1)$ or $\bar{s}_t$ must be added by $\Delta\phi(1)$ or $\Delta\bar{s}_t$ depended on which parameters is varied.
5. Repeat steps 2-4 and create the load-deflection curves.

6. Results and discussion

As mentioned in section 1, there are two processes for studying this problem. The first process is slackening-twist process in which the axial force is applied first and then the torque is applied at the sleeve end for studying the behavior of three-dimensional elastica. The second process is twist-slackening process in which the torque is applied before the axial force. In this process, the effect of

variable-arc-length to behavior of rod will be captured. In both processes, the total arc-length will be limited within the range $1<\bar{s}_t<10$ since in practical considerations, the total arc-length of marine risers is rarely found to be 10 times greater than its span length ($\bar{s}_t>10$) and it is sufficient to observe the global behavior of VAL clamped elastica.

6.1 Slackening-twist process

First, the VAL elastica is compressed by axial force in which the relationship between axial force and total arc-length is shown in Fig. 1. As it can be seen in Fig. 1, the axial force decreases as total arc-length increases. In contrast to the normal clamped elastica that total arc-length is fixed, the axial force must be increased in order to maintain the equilibrium configuration in deformed state. This can be concluded that planar VAL elastica with the inflection points exhibits the softening path while clamped elastica gives the hardening path.

Beginning with the deformed shapes in softening path of clamped VAL elastica, a torque is applied at the sleeve end of the elastica. The results are plotted in load-deflection diagram of torque $\bar{Q}$ and twist angle $\phi(1)$ shown in Fig. 4. To determine the stability properties of these curves, the fold rule initiated by Maddocks 1987 is utilized for predicting the stability of VAL elastica as well as in Heijden *et al.* 2003. They used the fold rule for evaluating the stability of clamped elastica. The fold rule stated that "If the real valued functional $-F_y$(i.e. $\partial F/\partial\lambda$) is chosen as the ordinate in a bifurcation diagram, then the lower branch of extremals in a fold opening to right, and the upper branch in fold opening to left can not represent local minima of functional F". For this study in Eq. (33), the functional Π obtained from Heijden and Thompson 2000 refers to the functional F in the fold rule statement.

$$\Pi=\frac{1}{2}\int(GJ\omega_1^2+EI\omega_2^2+EI\omega_3^2)ds+T(s_t-L)-Q\phi(1) \tag{33}$$

As it can be observed that the sign of axial force T and torque Q are different, then the stability properties in fold rule must be switched.

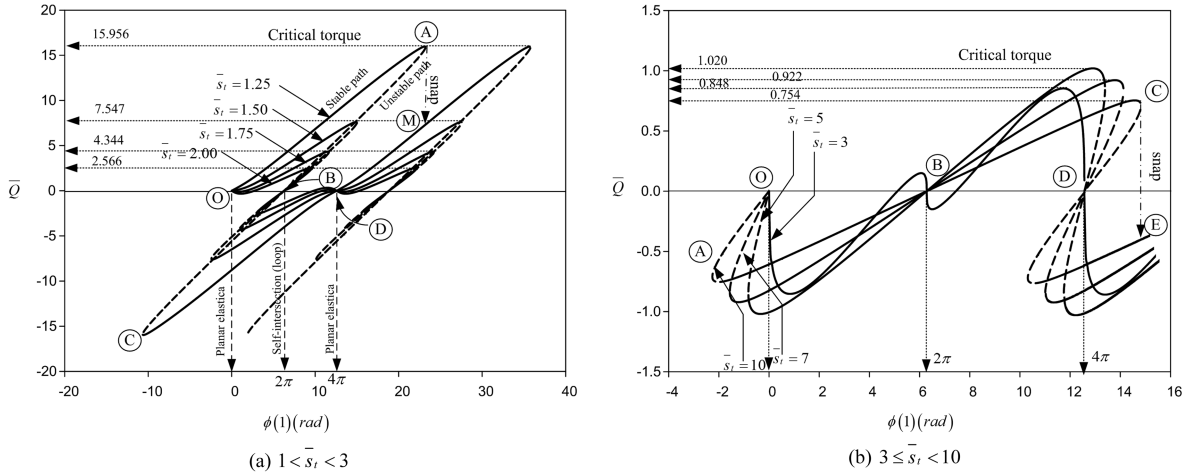

(a) $1<\bar{s}_t<3$ (b) $3\le\bar{s}_t<10$

Fig. 4 Load-deflection curve between torque $\bar{Q}$ and twist angle $\phi(1)$ at various values of total arc-length $\bar{s}_t$: (a) $1<\bar{s}_t<3$; (b) $3\le\bar{s}_t<10$: solid line is stable path, dash line is unstable path

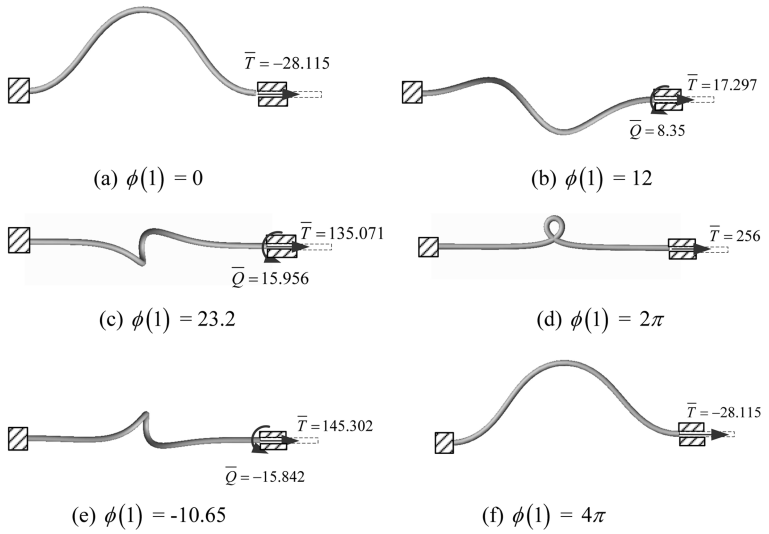

Fig. 5 Equilibrium configurations of VAL elastica for $\bar{s}_t$ = 1.25: (a) $\phi(1) = 0$, (b) $\phi(1) = 12$, (c) $\phi(1) = 23.2$, (d) $\phi(1) = 2\pi$; (e) $\phi(1) = -10.65$, (f) $\phi(1) = 4\pi$

The results are plotted in load-deflection curves of torque $\bar{Q}$ and twist angle $\phi(1)$ in Figs. 4(a) and (b). Two behaviors of clamped VAL elastica will be elucidated. One is the case of total arc-length $1 < \bar{s}_t < 3$ and the other is for total arc-length $3 < \bar{s}_t < 10$. In the former case in Fig. 4(a), the equilibrium paths are initiated from point O that matches with the planar elastica (see Fig. 5(a)). Using the fold rule and considering the minus sign in Eq. (33), the stability properties of load-deflection curves between torque $\bar{Q}$ and twist angle $\phi(1)$ must be opposite to fold rule. Considering path OABC, from point O to A, the equilibrium path is stable in which the torque $\bar{Q}$ increases as the twist angle $\phi(1)$ increases. By continuously increasing of the applied torque on path OA, the elastica forms the equilibrium shapes in three-dimensional space (Figs. 5(b) and (c)). However the equilibrium paths are not monotonic, they have a limit load points (e.g. point A), the critical point, depending on values of total arc-length $\bar{s}_t$. The configuration shape at point A is presented in Fig. 5(c). By observing the peak values of torque $\bar{Q}$ in each curve from Fig. 4, the critical load is decreased considerably when total arc-length $\bar{s}_t$ is increased. This indicates that when flexible marine riser is substantially slackened, the riser can easily form the loop shape. At point A, if the twist angle $\phi(1)$ still increases, the elastica will lose its stability by snap-through phenomenon. Unless the decrease of twist angle along unstable path ABC results in loop formation of elastica at point B presented in Fig. 5(d) where the applied torque becomes zero and twist angle $\phi(1)$ is rotated at 2π. Regardless of the effect of self-contact, the VAL elastica continuously move through the intersection point until reaches point C (see Fig. 5(e)). After point C, the equilibrium path displays stable state again and the equilibrium configuration along this path unfolds to planar elastica with inflection points at twist angle $\phi(1) = 4\pi$. The behavior of twisted elastica will be repeated to path OABCD again after this point or we may state that the load-deflection curve $\bar{Q} - \phi(1)$ has the period at $\pm 4\pi$. From previous results, the planar elastica occurs when twist angle $\phi(1)$ equals 0, 2π and 4π. Hence, we may summarize that at twist angle $\phi(1) = \pm 2n\pi$ where n is an integer odd number, the elastica is deformed as planar elastica with inflection points but if n is integer even number (include zero), the elastica is deformed as planar elastica without inflection point.

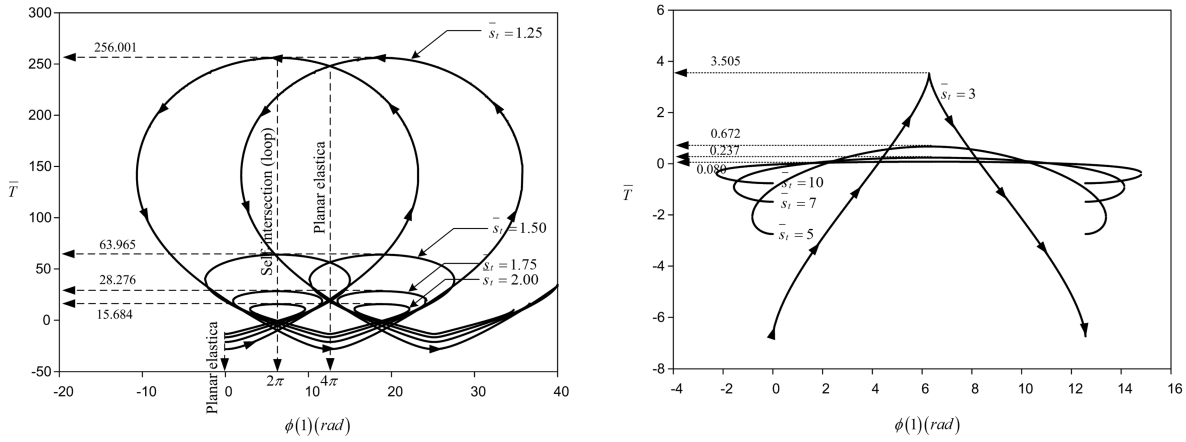

(a) $1 < \bar{s}_t < 3$ (b) $3 \le \bar{s}_t < 10$

Fig. 6 Relationship between axial force $\bar{T}$ and twist angle $\phi(1)$ at various values of total arc-length $\bar{s}_t$: (a) $1 < \bar{s}_t < 3$, (b) $3 \le \bar{s}_t < 10$

By considering the axial force $\bar{T}$, first the compressive force must be exerted in order to obtain the deformed configuration before twist process. From diagram in Fig. 6(a), during twisting process, the compressive force decreases rapidly and become tensile force at a certain value of twist angle $\phi(1)$. The axial force is developed along the curve in Fig. 6(a). The tensile force $\bar{T}$ increases as twist angle ϕ increases until it reaches critical point, after that the twist angle $\phi(1)$ decreases but the tensile force still increases to the maximum tension corresponding to the loop shape of elastica. After that the axial force decreases continuously to the minimum point which is same value as the beginning.

For the case of total arc-length in the range $3 < \bar{s}_t < 10$, the equilibrium path emanated from point O is unstable path (see Fig. 4(b)) and this path becomes stable at minimum the turning point (critical point A). Beyond this turning point, the elastica folds into the loop shape (point B) at twist angle $\phi(1) = 2\pi$. By increasing the twist angle $\phi(1)$, the applied torque is developed until it reaches the critical point at positive side (point C) after that the equilibrium path is changed to unstable path again in which the torque $\bar{Q}$ drops to zero for twist angle $\phi(1) \to 4\pi$. At this point, the elastica returns to the original shape (planar elastica with inflection points). It is worth noticing that the snap-through phenomenon may occur at point C if the twist angle $\phi(1)$ is still increased. The diagram of axial force $\bar{T}$ and twist angle $\phi(1)$ shown in Fig. 6(b) seems to be different from the case $1 < \bar{s}_t < 3$ but the main features are still unchanged.

Addressing to the critical torque $\bar{Q}_{cr}$ and the maximum axial force $\bar{T}_{\max}$ in Table 2 and Fig. 7, it can be seen that the critical torque decreases as total arc-length $\bar{s}_t$ increases. However, in some values of total arc-length (e.g. $\bar{s}_t = 4$ and 5), the critical torque slightly increases and it begins to

Table 2 Critical torque $\bar{Q}_{cr}$ and maximum axial force $\bar{T}_{\max}$

Loads	$\bar{s}_t$									
	1.2	2	3	4	5	6	7	8	9	10
$\bar{Q}_{cr}$	19.994	2.566	0.853	1.008	1.02	0.979	0.922	0.862	0.806	0.753
$\bar{T}_{\max}$	400.109	15.684	3.508	1.361	0.672	0.381	0.238	0.158	0.110	0.080

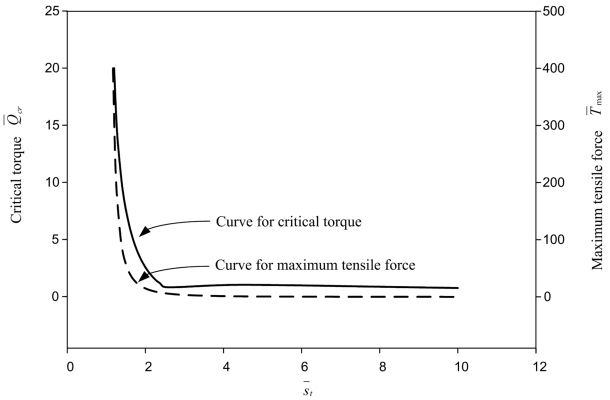

Fig. 7 Critical torque $\overline{Q}_{cr}$ and maximum axial force $\overline{T}_{\max}$ at various total arc-length $\overline{s}_t$

drop again for $\overline{s}_t > 5$. Above the critical torque, there is no equilibrium state. In case of maximum axial force $\overline{T}_{\max}$, it decreases rapidly when the total arc-length $\overline{s}_t$ increases. It is important to note that the critical torque and maximum tension are occurred at different situations. The critical torque is occurred before elastica jumps into the loop formation but the maximum tension is occurred when elastica is the loop configuration.

6.2 Twist- slackening process

By keeping the twist angle as a constant and then applying the axial force, the results from this process are shown in Fig. 8. The effects of variable-arc-length to the axial force are presented in Fig. 8. The buckling equation derived by Heijden *et al.* 2003 is employed to this problem since in the case of small deflection there is no difference between calmped VAL elastica and normal clamped elastica. Thus, the buckling equation from Heijden *et al.* 2003 is quoted again in following equation for giving the initial information about buckling load.

$$\cos(\pi\sqrt{m^2-4t}) - \cos(\pi m) = 2\pi t\left(\frac{\sin(\pi\sqrt{m^2-4t^2})}{\sqrt{m^2-4t^2}}\right) \tag{34}$$

where

$$m = \frac{QL}{4\pi EI}, \quad t = \frac{TL^2}{4\pi^2 EI} \tag{35a,b}$$

Regarding to Fig. 8, four different behaviors of elastica according to $\phi(1) = 0$, $0 < \phi(1) < 2\pi$, $\phi(1) = 2\pi$ and $\phi(1) > 2\pi$ can be captured. In the case of twist angle $\phi(1) = 0$, the elastica deforms as a stable planar elastica from total arc-length $1 < \overline{s}_t \le 3$. At total arc-length $\overline{s}_t = 3$, there is a bifurcation point B_1 in which two equilibrium paths emanate from this point. One is unstable path (dash line) according to planar elastica and the other is stable path (solid line) in which the elastica deforms in three-dimensional space. In addition, this branch is a connecting branch between planar elastica with inflection points and planar elastica without inflection point (loop shape). On the other word, the planar elastica with inflection points moving along this path will form into loop shape for total arc-length $\overline{s}_t \to 10$. For the case of $0 < \phi(1) < 2\pi$, the equilibrium path is stable path. The axial force $\overline{T}$ decreases as total arc-length $\overline{s}_t$ increases. Under slackening process, the

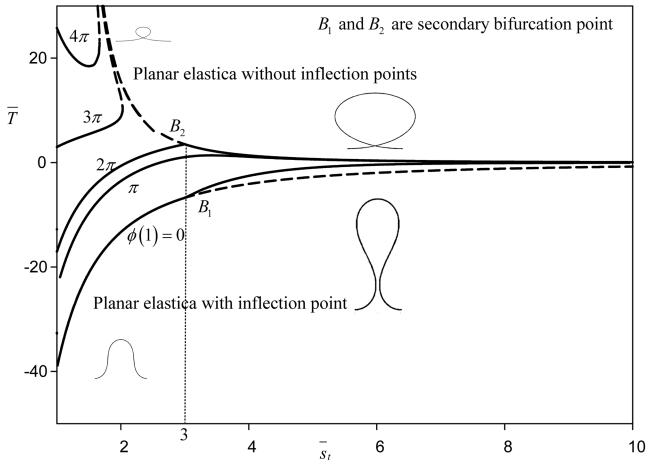

Fig. 8 Load-deflection curves between axial force $\bar{T}$ and total arc-length $\bar{s}_t$ at various values of twist angle $\phi(1) = 0$, π, 2π, 3π and 4π: solid line is stable path, dash line is unstable path

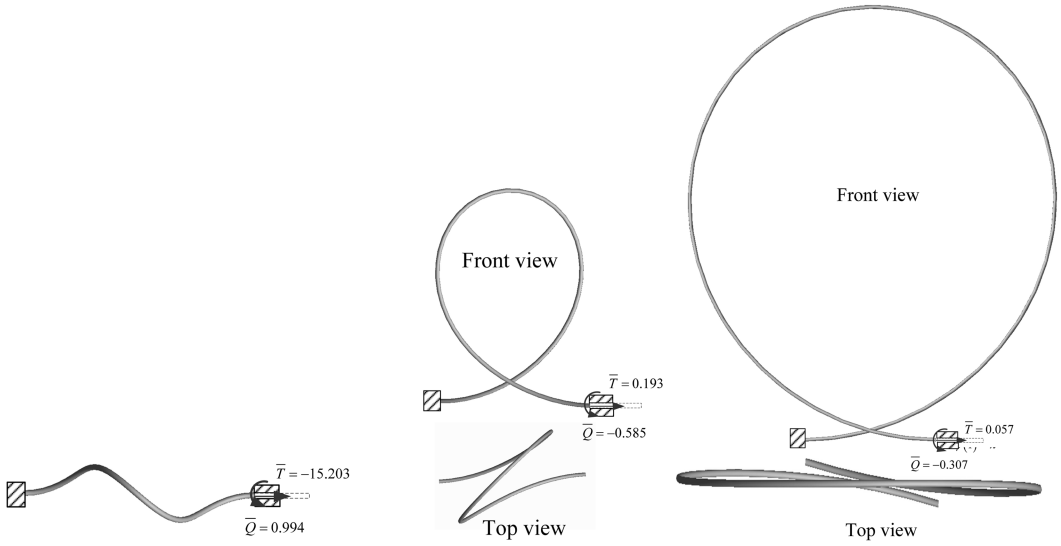

(a) $\bar{s}_t = 1.5$ (b) $\bar{s}_t = 4.05$ (c) $\bar{s}_t = 10$

Fig. 9 Equilibrium configuration of VAL elastica in slackening process for the case of $\phi(1) = \pi$: (a) $\bar{s}_t = 1.5$, (b) $\bar{s}_t = 4.05$, (c) $\bar{s}_t = 10$

VAL elastica has the trend to form the loop at a certain value of total arc-length $\bar{s}_t$. The equilibrium shapes of this case are shown in Fig. 9. In case of twist angle $\phi(1) = 2\pi$, the equilibrium path is similar to the case of $0 < \phi(1) < 2\pi$ but this path goes to connect with path of planar elastica without inflection point at $\bar{s}_t = 3$ (secondary bifurcation point B_2) which contains unstable path for the upper branch and stable path for the lower branch. Following the unstable path, the tension $\bar{T}$ becomes larger value according to smaller loop of elastica or the tension $\bar{T}$ is decreased along the stable path according to the larger loop of elastica. In the third case $\phi(1) > 2\pi$, the lower branch of

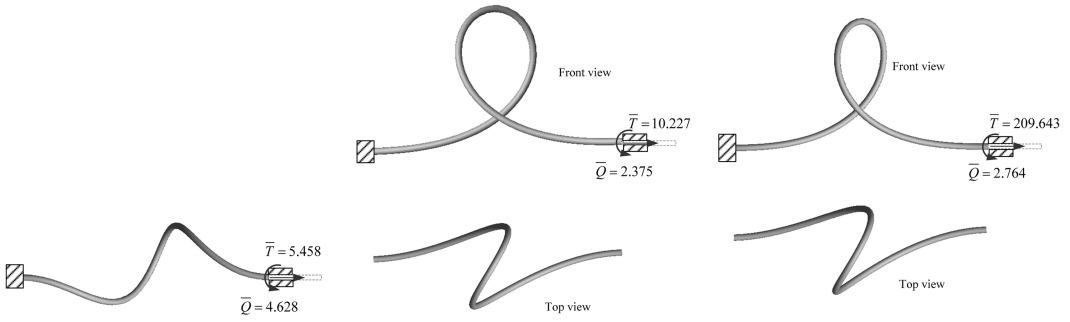

Fig. 10 Equilibrium configuration of VAL elastica in slackening process for the case of $\phi(1) = 3\pi$: (a) $\phi(1) = 1.5$, (b) $\phi(1) = 2.028$, (c) $\phi(1) = 1.275$

equilibrium path is the stable path while the upper branch is unstable path. The elastica can form the loop shape by moving on this unstable path. The total arc-length for this case has the limitation point depended on value of twist angle $\phi(1)$. For the example, the total arc-length $\bar{s}_t$ is never larger than 2.0279 and 1.6668 for twist angle $\phi(1) = 3\pi$ and 4π, respectively. The equilibrium configurations for this case are presented in Fig. 10.

7. Conclusions

From the results, the investigation of VAL clamped elastica can be summarized as follows:

1. In slackening-twist process, the two behaviors depended on the value of total arc-length $\bar{s}_t$ of elastica are captured. For total arc-length $1 < \bar{s}_t < 3$, the equilibrium path is initiated with stable path until it reaches the critical point in which the raising of twist angle $\phi(1)$ leads to snap-through phenomenon. But for total arc-length $3 < \bar{s}_t < 10$, the first branch is unstable path and it switches into stable path at the turning point. The snap-through phenomenon for this case appears during the elastica is twisted larger than 4π. In case of total arc-length $\bar{s}_t = 3$, the equilibrium path seems to be in the stage of the transition from the case $1 < \bar{s}_t < 3$ to the case $3 < \bar{s}_t < 10$.
2. In twist-slackening process, the stability of clamped elastica is divided into four cases. For the first case $\phi(1) = 0$, the elastica deforms as a planar and stable elastica for total arc-length $1 < \bar{s}_t < 3$. For $\bar{s}_t > 3$, there is a secondary bifurcation point where two different paths are emanated from this point. One is unstable according to planar elastica and the other is stable path corresponding with twisted elastica. The twist angle $0 < \phi(1) < 2\pi$, the second case, the buckled elastica exhibits only the stable equilibrium shape for $1 < \bar{s}_t < 10$. In the third case, $\phi(1) = 2\pi$, the elastica also deforms in stable shape as well as the two former cases. However, it contains the secondary bifurcation point at total arc-length $\bar{s}_t = 3$. At this point, the elastica is in transition stage which may become stable or unstable depending on the applied tension (or total arc-length $\bar{s}_t$). The final case is for $\phi(1) > 2\pi$ in which the elastica is deformed in stable state at first and it becomes unstable at the turning point.
3. The loop formation occurs when twist angle $\phi(1)$ is rotated at an angle 2π and becomes the original shape when $\phi(1) = 4\pi$ for every value of total arc-length $\bar{s}_t$.

4. The critical torque $\overline{Q}_{cr}$ drops considerably as the total arc-length increases. However the critical torque $\overline{Q}_{cr}$ is slightly increased at some values of total arc-length $\overline{s}_t$ and then it gradually decrease as total arc length $\overline{s}_t$ increases. For the maximum axial force $\overline{T}_{\max}$, it decreases monotonically as total arc-length $\overline{s}_t$ increases.

Acknowledgements

The authors gratefully gratitude Thailand Research Fund (TRF) for financial support under grants PHD/0045/2548.

References

Atanackovic, T.M. and Glavardanov, V.B. (2002), "Buckling of a twisted and compressed rod", *Int. J. Solid Struct.*, **39**(11), 2987-2999.

Balaeff, A., Mahadevan, L. and Schulten, K. (2006), "Modeling DNA loops using the theory of elasticity", *Phys. Rev. E*, **73**(3), 031919(23).

Benecke, S. and Vuuren, J.H.V. (2005), "Modelling torsion in an elastic cable in space", *Appl. Math. Model.*, **29**(2), 117-136.

Chucheepsakul, S. Buncharoen, S. and Huang, T. (1995), "Elastica of simple variable-arc-length beam subjected to end moment", *J. Eng. Mech.*, ASCE, **121**(7), 767-772.

Chucheepsakul, S. and Huang, T. (1992), "Finite element solution of large deflection analysis of a class of beam", *Proc. Comput. Meth. Eng.*, **1**, 45-50.

Chucheepsakul, S. and Huang, T. (1997), "Finite-element solution of variable-arc-length beams under a point load", *J. Eng. Mech.*, ASCE, **123**(7), 968-970.

Chucheepsakul, S. and Monprapussorn, T. (2000), "Divergence instability of variable-arc-length elastica pipes transporting fluid", *J. Fluids Struct.*, **14**(6), 895-916.

Chucheepsakul, S. and Monprapussorn, T. (2001), "Nonlinear buckling of marine elastica pipes transporting fluid", *Int. J. Struct. Stabil. Dyn.*, **1**(3), 333-365.

Chucheepsakul, S. and Phungpaigram, B. (2004), "Elliptic integral solutions of variable-arc-length elastica under an inclined follower force", *Z. Angew Math. Mach. (ZAMM)*, **84**(1), 29-38.

Chucheepsakul, S., Thepphitak, G. and Wang, C.M. (1996), "Large deflection of simple variable-arc-length beam subjected to a point load", *Struct. Eng. Mech.*, **4**(1), 49-59.

Chucheepsakul, S., Thepphitak, G. and Wang, C.M. (1997), "Exact solutions of variable-arc-length elastica under moment gradient", *Struct. Eng. Mech.*, **5**(5), 529-539.

Chucheepsakul, S., Wang, C.M., He, X.Q. and Monprapussorn, T. (1999), "Double curvature bending of variable-arc-length elasticas", *J. Appl. Mech.*, ASME, **66**(1), 87-94.

Clebsch, A. (1862), *Theorie der Elastictät Fester Körper*, *B.G.* Teubner, Leipzig.

Coleman, B.D. and Swigon, D. (2000), "Theory of supercoiled elastic rings with self-contact and its application to DNA plasmids", *J. Elasticity*, **60**(3), 173-221.

Coleman, B.D., Tobias, I. and Swigon, D. (1995), "Theory of the influence of the end conditions on self-contact in DNA loops", *J. Chem. Phys.*, **103**(20), 9101-9109.

Cosserat, E. and Cosserat, F. (1907), "Sur la statique de la ligne déformable", *C.R. Acad. Sci. Paris*, **145**, 1409-1412.

Coyne, J. (1990), "Analysis of the formation and elimination of loops in twisted cable", *IEEE J. Oceanic Eng.*, **15**(2), 72-83.

Goyal, S., Perkins, N.C. and Lee, C.L. (2005), "Nonlinear dynamics and loop formation in kirchhoff rods with implications to the mechanics of DNA and cables", *J. Comput. Phys.*, **209**(1), 371-389.

He, X.Q., Wang, C.M. and Lam, K.Y. (1997), "Analytical bending solutions of elastica with one end held while

the other end portion slides on the friction support", *Arch. Appl. Mech.*, **67**(8), 543-554.
Katopodes, F.V., Barber, J.R. and Shan, Y. (2001), "Torsional deformation of an endoscope probe", *P. Roy. Soc. London,* **457**(2014), 2491-2506.
Kirchhoff, G. (1859), "Über das gleichgewicht und die bewegung eines unendlich dünnen elastichen stabes", J. F. *Reine. Angew. Math. (Crelle)*, **56**, 285-313.
Love, A.E.H. (1892), *A Treatise on the Mathematical Theory of Elasticity*, First Edition, Cambridge University Press.
Lu, C.L. and Perkins, N.C. (1994), "Nonlinear spatial equilibria and stability of cables under uni-axial torque and thrust", *J. Appl. Mech.,* ASME, **61**(4), 879-886.
Lu, C.L. and Perkins, N.C. (1995), "Complex spatial equilibria of U-joint supported cables under torque, thrust and self-weight", *Int. J. Non-linear Mech.*, **30**(3), 271-285.
Maddocks, J.H. (1987), "Stability and folds", *Arch. Ration. Mech. Anal.*, **99**(4), 301-327.
Miyazaki, Y. and Kondo, K. (1997), "Analytical solution of spatial elastica and its application to kinking problem", *Int. J. Solids Struct.*, **34**(27), 3619-3636.
Nikravesh, P.E. (1988), *Computer-Aided Analysis of Mechanical Systems*, Prentice Hall, New Jersey.
Pulngern, T., Halling, M.W. and Chucheepsakul, S. (2005), "Large deflections of variable-ARC-length beams under uniform self weight: Analytical and experimental", *Struct. Eng. Mech.*, **19**(4), 413-423.
van der Heijden, G.H.M., Neukirch, S. and Thompson, J.M.T. (2003), "Instability and self-contact phenomena in the writhing of clamped rods", *Int. J. Mech. Sci.*, **45**(1), 161-196.
van der Heijden, G.H.M. and Thompson, J.M.T. (2000), "Helical and localised buckling in twisted rods: A unified analysis of the symmetric case", *Nonlinear Dyn.*, **21**(1), 71-99.
Wang, C.M., Lam, K.Y. and He, X.Q. (1998), "Instability of variable arc-length elastica under follower force", *Mech. Res. Commun.*, **25**(2), 189-194.
Wang, C.M., Lam, K.Y., He, X.Q. and Chucheepsakul, S. (1997), "Large deflections of an end supported beam subjected to a point load", *Int. J. Nonlinear Mech.*, **32**(1), 63-72.
Zhang, X. and Yang, J. (2005), "Inverse problem of elastica of variable-arc-length beam subjected to a concentrated load", *Acta Mech. Sinica*, **21**(5), 444-450.